Tuning arousal with optogenetic modulation of locus coeruleus neurons

Matthew E Carter[1,2], Ofer Yizhar[3], Sachiko Chikahisa[4,5], Hieu Nguyen[2], Antoine Adamantidis[2], Seiji Nishino[4], Karl Deisseroth[1,3] & Luis de Lecea[1,2]

Neural activity in the noradrenergic locus coeruleus correlates with periods of wakefulness and arousal. However, it is unclear whether tonic or phasic activity in these neurons is necessary or sufficient to induce transitions between behavioral states and to promote long-term arousal. Using optogenetic tools in mice, we found that there is a frequency-dependent, causal relationship among locus coeruleus firing, cortical activity, sleep-to-wake transitions and general locomotor arousal. We also found that sustained, high-frequency stimulation of the locus coeruleus at frequencies of 5 Hz and above caused reversible behavioral arrests. These results suggest that the locus coeruleus is finely tuned to regulate organismal arousal and that bursts of noradrenergic overexcitation cause behavioral attacks that resemble those seen in people with neuropsychiatric disorders.

The locus coeruleus is a noradrenergic brainstem structure that is thought to be important for promoting arousal[1–5]. Neurons in the locus coeruleus fire tonically at 1–3 Hz during awake states, fire less during non–rapid eye movement (NREM) sleep and are virtually silent during REM sleep[6–8]. The locus coeruleus also fires phasically in short bursts of 8–10 Hz during the presentation of salient stimuli that prolong wake states[7,9]. Importantly, alterations in discharge rate precede changes in sleep-to-wake transitions[6,8,9]. However, it is unclear whether this activity is causal or submissive, and the specific contributions of tonic and phasic activity to the modulation of arousal states are unknown.

The small size, unique morphology and proximity to neighboring brain structures of the locus coeruleus have made it difficult to use traditional pharmacological and electrical techniques to show that it has a causal role in promoting and maintaining arousal[1,2]. Physical lesions of the locus coeruleus do not elicit consistent changes in cortical electroencephalography (EEG) or behavioral indices of arousal[10–12]. Genetic ablation of dopamine beta-hydroxylase, which is required for norepinephrine synthesis, also does not disrupt sleep-wake states[13]. However, central injections of pharmacological antagonists of noradrenergic receptors[14] or agonists of inhibitory autoreceptors[15] have substantial sedative effects. By contrast, central administration of norepinephrine directly into the ventricles or forebrain promotes wakefulness[16,17]. Stimulation of neurons in the locus coeruleus using local microinjections of the cholinergic agonist bethanechol produces rapid activation of the forebrain EEG in halothane-anesthetized rats[18]. Together, these results imply that the locus coeruleus is involved in promoting arousal. However, new tools are needed to selectively manipulate the discharge activity of the locus coeruleus in freely moving, behaving mice at timescales that are relevant to natural sleep-wake events.

The recent development of optogenetic tools[19,20] has provided a valuable opportunity to inhibit or stimulate activity in genetically targeted neural populations with high spatial and temporal precision[21,22]. Therefore, to identify a conclusive, causal role for the locus coeruleus norepinephrine system in promoting and maintaining wakefulness, we inhibited locus coeruleus neurons with halorhodopsin (eNpHR; a chloride pump that is sensitive to yellow light)[23,24] or stimulated them with channelrhodopsin-2 (ChR2; a cation channel that is sensitive to blue light)[25]. We found that the locus coeruleus was necessary to maintain wake episodes but that its inhibition did not increase the duration of sleep episodes. Stimulation caused immediate sleep-to-wake transitions, extending the duration of wakefulness in a manner that was consistent with sleep deprivation. The probability of wakefulness during stimulation was finely tuned to both light pulse frequency and the duration of stimulation, indicating that the sleep-wake state of an animal is highly sensitive to activity in the locus coeruleus at a scale of single action potentials. We also found that sustained (10–15 s) high-frequency (>5 Hz) stimulation caused reversible behavioral arrests that had, to our knowledge, not previously been reported to result from stimulation of the locus coeruleus, which suggests a potential mechanism for the behavioral arrests that occur in some neuropsychiatric disorders.

RESULTS
Genetic targeting of locus coeruleus neurons
We genetically targeted locus coeruleus neurons by stereotaxically injecting a Cre-recombinase-dependent adeno-associated virus (rAAV)[26,27] into knockin mice that selectively expressed Cre in tyrosine hydroxylase–expressing neurons[28] (**Supplementary Fig. 1**). We validated the specificity and efficiency of transgene expression by

[1]Neurosciences Program, Stanford University, Stanford, California, USA. [2]Department of Psychiatry and Behavioral Sciences, Stanford University, Stanford, California, USA. [3]Department of Bioengineering, Stanford University, Stanford, California, USA. [4]Sleep & Circadian Neurobiology Laboratory, Stanford University, Stanford, California, USA. [5]Department of Integrative Physiology, Institute of Health Biosciences, University of Tokushima Graduate School, Tokushima, Japan. Correspondence should be addressed to L.d.L. (llecea@stanford.edu).

Figure 1 Specific and efficient functional expression of optogenetic transgenes in locus coeruleus neurons. (**a**) Representative photomicrographs depicting tyrosine hydroxylase (TH) immunoreactivity (left column, red), viral eYFP expression (center column, green) and merged images (right column) from an animal unilaterally injected with EF1α::eYFP rAAV virus into the left locus coeruleus. Top row, global expression in a coronal section counterstained with DAPI (scale bar, 100 μm); middle row, expression in the full locus coeruleus (scale bar, 25 μm); bottom row, individual neurons (scale bar, 5 μm). (**b**) Quantification of co-expression of eYFP and TH immunofluorescence from EF1α::eYFP transduced mice ($n = 4$) in 30-μm brain sections from the rostral-to-caudal ends of the locus coeruleus (anteroposterior, −5.20 to −5.80). Cell counts are represented as mean ± s.d. Inset represents the statistics of the total coexpression. (**c**) Voltage clamp recording of a neuron expressing eNpHR-eYFP in brainstem slice showing outward current in response to yellow light. (**d**) Voltage clamp recording of a neuron expressing ChR2-eYFP in brainstem slice showing inward current in response to blue light. (**e**) Action potential trains recorded under current clamp conditions from a neuron expressing eNpHR-eYFP in brainstem slice for 5 s (top) or 1 min (bottom). (**f**) Blue-light pulse trains (10 ms per pulse) evoked action potential trains at various frequencies in neurons expressing ChR2-eYFP. (**g**) Efficiency of action potential trains evoked by blue light pulses in neurons expressing ChR2-eYFP. Data represent mean probability ± s.e.m. from $n = 6$ neurons.
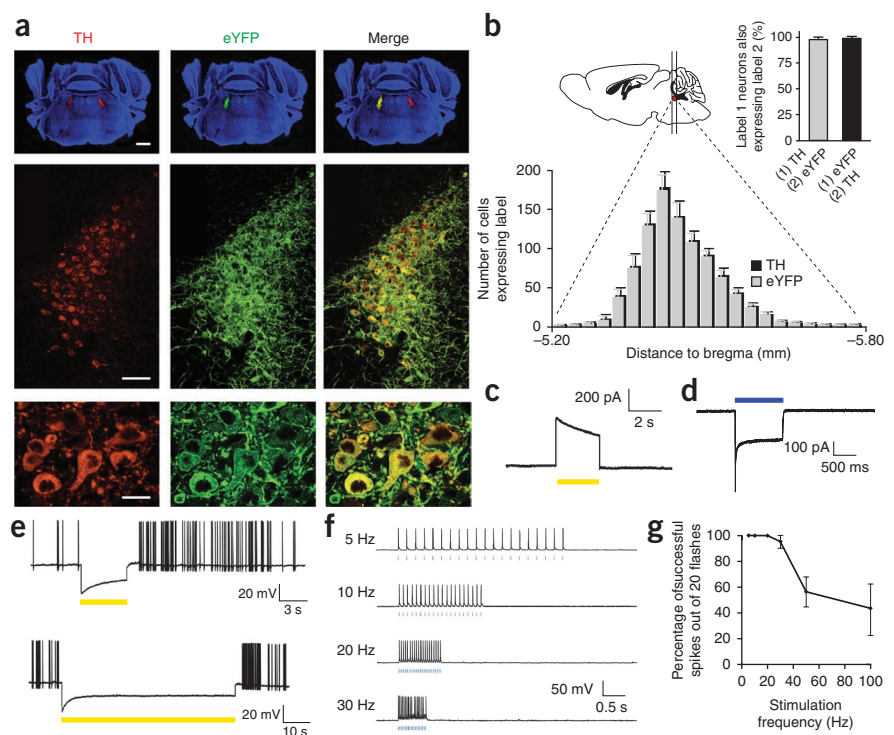
unilaterally injecting virus that encoded enhanced yellow fluorescent protein (eYFP) alone (control), eYFP-eNpHR or eYFP-ChR2 into the locus coeruleus region[29] and comparing the expression of viral eYFP with tyrosine hydroxylase immunofluorescence. eYFP fluorescence was detected throughout the entire locus coeruleus but not in neighboring noradrenergic or dopaminergic regions (**Fig. 1a** and **Supplementary Fig. 2**). Out of 3,463 neurons that expressed tyrosine hydroxylase ($n = 4$ mice), 98.1 ± 1.9% also expressed eYFP (mean ± s.e.m.; **Fig. 1b**). Conversely, 97.9 ± 2.9% of eYFP-positive cells also expressed tyrosine hydroxylase (**Fig. 1b**), which showed that viral targeting of the locus coeruleus was specific.

To test the functional expression of optogenetic transgenes in locus coeruleus neurons, we recorded from eYFP-positive neurons in acute brainstem slices using the whole-cell patch clamp technique. In voltage-clamp mode, we found that neurons that had been transduced with eNpHR showed rapid outward photocurrents upon illumination with yellow light (**Fig. 1c**), with a peak of 435.5 ± 44.2 pA and a steady state of 302.2 ± 65.8 pA ($n = 5$ cells). By contrast, photostimulation of ChR2-transduced neurons with blue light caused an inward steady-state current of 321 ± 50 pA ($n = 6$ cells; **Fig. 1d**). In current-clamp experiments, eNpHR-transduced neurons were hyperpolarized by yellow light, which completely blocked endogenous spontaneous action potentials (**Fig. 1e**). In locus coeruleus neurons that had been transduced with ChR2, 10-ms pulses of blue light caused action potentials at 1–30 Hz (**Fig. 1f**). The efficiency of ChR2-mediated spikes decreased with increasing frequency, with 100% efficiency at 20 Hz and below (**Fig. 1g**). These *in vitro* results show that rAAV-mediated expression of eNpHR or ChR2 can inhibit or stimulate action potentials, respectively, in locus coeruleus neurons.

To modulate the neural activity of the locus coeruleus *in vivo*, we bilaterally injected rAAV into each locus coeruleus region

(**Supplementary Fig. 1c**) and implanted a bilateral cannula for subsequent light delivery. We placed EEG and electromyographic (EMG) electrodes in the skull and neck musculature, respectively, for sleep-wake analysis (**Supplementary Fig. 3**). Initial sleep recordings showed that there was no difference in baseline sleep architecture between virally transduced mice and control mice ($n = 4$ mice per condition; **Supplementary Fig. 4**).

To ensure the correct placement of cannulae and fiber optic cables, we applied long-term photostimulation (10-ms pulses at 3 Hz for 1 h) to the left locus coeruleus in ChR2-eYFP–transduced mice or eYFP–transduced control mice ($n = 4$ mice per condition) during the inactive (light) period and detected the presence of c-Fos, an indirect marker of neural activity (**Supplementary Fig. 5**). There were significantly more tyrosine hydroxylase–positive cells that also expressed c-Fos in ChR2-eYFP mice (64.7 ± 13.6%) than in eYFP mice (17.2 ± 7.2%) ($P < 0.001$). Furthermore, c-Fos was expressed throughout the anteroposterior length of the locus coeruleus (**Supplementary Fig. 5c**), showing that our *in vivo* light delivery procedure could accurately stimulate the entire population of locus coeruleus neurons.

To validate eNpHR-mediated inhibition of the locus coeruleus *in vivo*, we tested the effect of photoinhibition on norepinephrine content in the prefrontal cortex, which receives noradrenergic projections only from the locus coeruleus. We delivered constant yellow light to the locus coeruleus in freely moving mice transduced with eNpHR-eYFP or eYFP ($n = 4$ mice per condition) during the active (dark) period for 10 min while simultaneously using microdialysis to sample extracellular fluid from the prefrontal cortex. Continuous photoinhibition for 10 min significantly decreased cortical norepinephrine in eNpHR-eYFP mice ($P < 0.001$), but not in eYFP control mice (**Supplementary Fig. 6**), showing that eNpHR-mediated photoinhibition is effective *in vivo*.
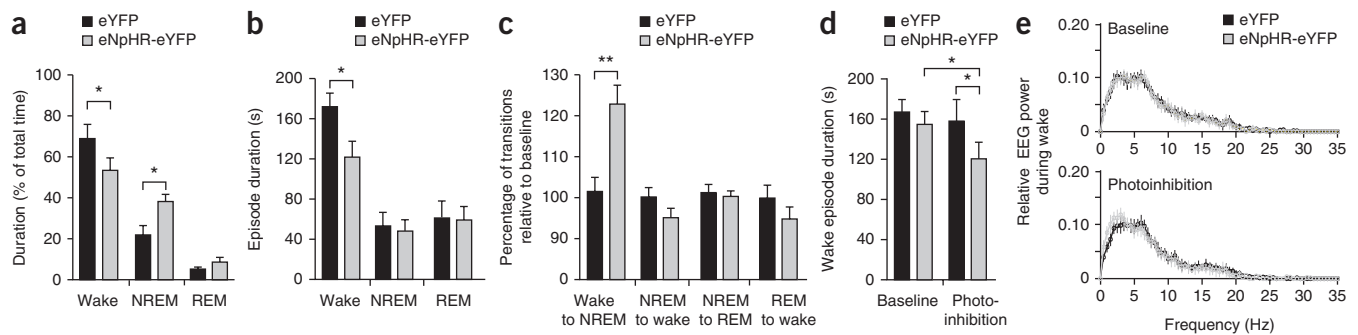
1527

Figure 2 Photoinhibition of locus coeruleus neurons causes a reduction in the duration of wakefulness. (**a**) The percentage of time spent awake, in NREM sleep and in REM sleep during 1 h of photoinhibition in the active (dark) period. Data represent the mean ± s.e.m. of 6 separate 1-h sessions; $n = 6$ mice throughout. *$P < 0.05$, two-tailed Student's t test between transduced mice. (**b**) The duration of individual wake, NREM and REM episodes during 1 h of photoinhibition during the active period. *$P < 0.05$, two-tailed Student's t test between transduced mice. (**c**) The percentage of sleep state transitions relative to baseline levels during 1 h of photoinhibition during the active period. **$P < 0.001$, two-tailed Student's t test between transduced mice. (**d**) The duration of individual wake episodes in baseline versus photoinhibition conditions (20 episodes per mouse, $n = 6$ mice). *$P < 0.05$, two-way ANOVA between stimulation condition and viral transduction followed by Tukey post-hoc test. (**e**) Relative EEG power of wakefulness 80–120 s after wake onset in baseline (top) and photoinhibition (bottom) conditions. Data represent the mean ± s.e.m. relative power of 0.5-Hz binned frequencies (20 episodes per mouse, $n = 6$ mice).

Inhibition of the locus coeruleus reduces wakefulness

To determine whether neural activity in the locus coeruleus is necessary for promoting wakefulness, we tested the effect of long-term photoinhibition of the locus coeruleus (constant yellow light for 1 h) on sleep-wake architecture during the inactive and active periods. We found no significant difference between eNpHR-eYFP and eYFP control mice ($P > 0.05$, $n = 6$ mice per condition) in the total duration of wake or sleep states during the inactive period (**Supplementary Fig. 7**). However, eNpHR-eYFP mice showed a significant decrease in wakefulness ($P < 0.05$) and a significant increase in NREM sleep ($P < 0.05$) during the active period, compared with eYFP control mice (**Fig. 2a**). The duration of individual wake episodes was significantly lower during the active period in these mice ($P < 0.05$), but there was no significant change in

the duration of NREM or REM episodes ($P > 0.05$; **Fig. 2b**). We also found a significant increase in the number of wake-to-NREM transitions in eNpHR-eYFP mice ($P < 0.001$), but no increase in any other sleep-state transitions (**Fig. 2c**), suggesting that the locus coeruleus is necessary for maintaining the normal duration of wake episodes.

To study the effects of photoinhibition of the locus coeruleus specifically during wakefulness, we used real-time, online EEG analysis to restrict photoinhibition to epochs when the animal was awake. We found a significant reduction in wake episode duration in eNpHR-eYFP mice ($n = 6$) between baseline (no inhibition) and photoinhibition conditions ($P < 0.05$; **Fig. 2d**), but no significant reduction in wake duration in photoinhibited control mice ($P > 0.05$). The power spectrum of the cortical EEG toward the end
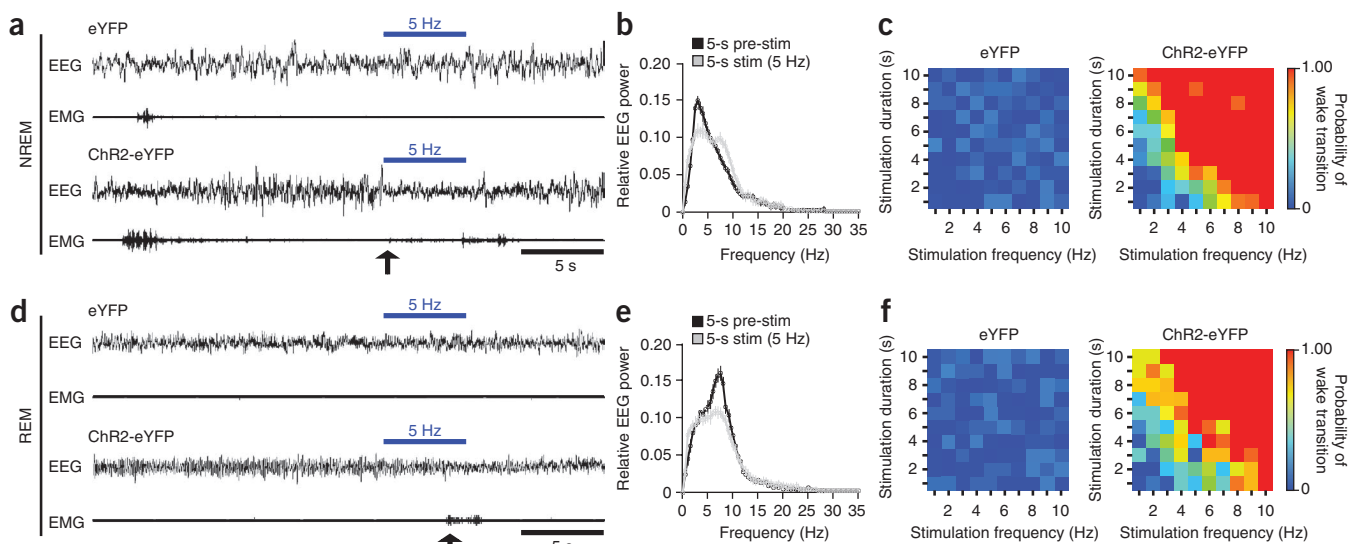

Figure 3 Photostimulation of locus coeruleus neurons causes immediate sleep-to-wake transitions. (**a–c**) Data from NREM sleep. (**d–f**) Data from REM sleep. (**a,d**) Representative traces of EEG/EMG recordings showing an immediate sleep-to-wake transition in NREM (**a**) or REM sleep (**d**) after acute photostimulation (10-ms pulses at 5 Hz for 5 s) of locus coeruleus neurons during the inactive period in a mouse transduced with ChR2-eYFP (bottom) but not in a mouse transduced with eYFP alone (top). Arrow, onset of sleep-to-wake transition. (**b,e**) Cortical EEG traces from ChR2-eYFP mice 5 s before the onset of stimulation (black) and 5 s into stimulation (gray). Quantification based on the average of 15 (**b**) or 8 (**e**) stimulations per mouse, $n = 6$ mice. (**c,f**) Heat maps showing the effects of photostimulation on NREM (**c**) or REM (**f**) sleep-to-wake transitions in eYFP ($n = 6$) or ChR2-eYFP ($n = 6$) transduced mice. Each square represents the mean probability of a sleep-to-wake transition within 10 s of the onset of stimulation. Data analysis is based on an average of 15 (**c**) or 8 (**f**) stimulations per condition per mouse.

of wake episodes (80–120 s from the onset of wakefulness in wake episodes lasting at least 120 s) showed no difference in the relative slow-wave activity (SWA, 0.5–4 Hz), a hallmark of sleep pressure, between eNpHR-eYFP and control mice in baseline (no inhibition) conditions (**Fig. 2e**). However, during photoinhibition, there was a significant increase in SWA in eNpHR-eYFP mice compared with control mice ($P < 0.05$, Student's t test), showing that eNpHR-eYFP mice are more likely to enter NREM sleep (**Fig. 2e**). These results suggest that the locus coeruleus is necessary for maintaining normal durations of wakefulness during the active period.

Stimulation of the locus coeruleus causes wake transitions

We next tested whether neurons in the locus coeruleus have a causal role in promoting wakefulness by testing the effect of photostimulation on sleep-to-wake transitions during the inactive period. We initially tested the effect of 5 Hz blue light stimulation for 5 s (10-ms pulses) during NREM sleep, always beginning stimulation trials 15 s after the onset of NREM sleep. Stimulation at these parameters reliably produced immediate sleep-to-wake transitions within 5 s of the onset of stimulation in ChR2-eYFP mice but not in eYFP control mice ($n = 6$ mice per condition; **Fig. 3a** and **Supplementary Movie 1**). In ChR2-eYFP mice, photostimulation produced immediate changes in the cortical EEG with a significant decrease in SWA ($P < 0.001$, two-tailed Student's t test between pre-stimulation and stimulation conditions; **Fig. 3b**). To determine the effects of various photostimulation frequencies and durations on sleep-to-wake transitions, we stimulated eYFP and ChR2-eYFP mice at frequencies of 1–10 Hz and

durations of 1–10 s (10-ms light pulses) and calculated the probability of an NREM-to-wake transition within 10 s of the onset of stimulation. The probability of an NREM-to-wake transition increased with stimulation frequency and duration in ChR2-eYFP mice, but not in control mice (**Fig. 3c**).

We also repeated the experiments above but studied the effect of photostimulation on REM sleep-to-wake transitions. Photostimulation at 5 Hz for 5 s (10-ms pulses) in ChR2-eYFP mice also caused immediate REM sleep-to-wake transitions (**Fig. 3d**), with immediate changes in the cortical EEG and a significant decrease in theta activity (4–9 Hz), which characterizes REM sleep ($P < 0.001$; two-tailed Student's t test between pre-stimulation and stimulation conditions; **Fig. 3e**). As in NREM sleep, the probability of sleep-to-wake transitions increased as we increased the frequency and duration of stimulation (**Fig. 3f**).

The relationship between the duration and frequency of stimulation that was necessary to cause a 100% probability of sleep-to-wake transitions was linear and inversely proportional during both NREM (**Fig. 3c** and **Supplementary Fig. 8a**) and REM sleep (**Fig. 3f** and **Supplementary Fig. 8b**). We also tested how many photostimulation pulses were required to induce a sleep-to-wake transition. As the frequency of stimulation increased, the number of pulses that were required to achieve a 100% probability of awakening decreased for both NREM (**Supplementary Fig. 8c**) and REM sleep (**Supplementary Fig. 8d**). As the duration of stimulation increased, the number of pulses that were required to achieve a 100% probability of awakening increased for both NREM (**Supplementary Fig. 8e**) and REM sleep (**Supplementary Fig. 8f**).
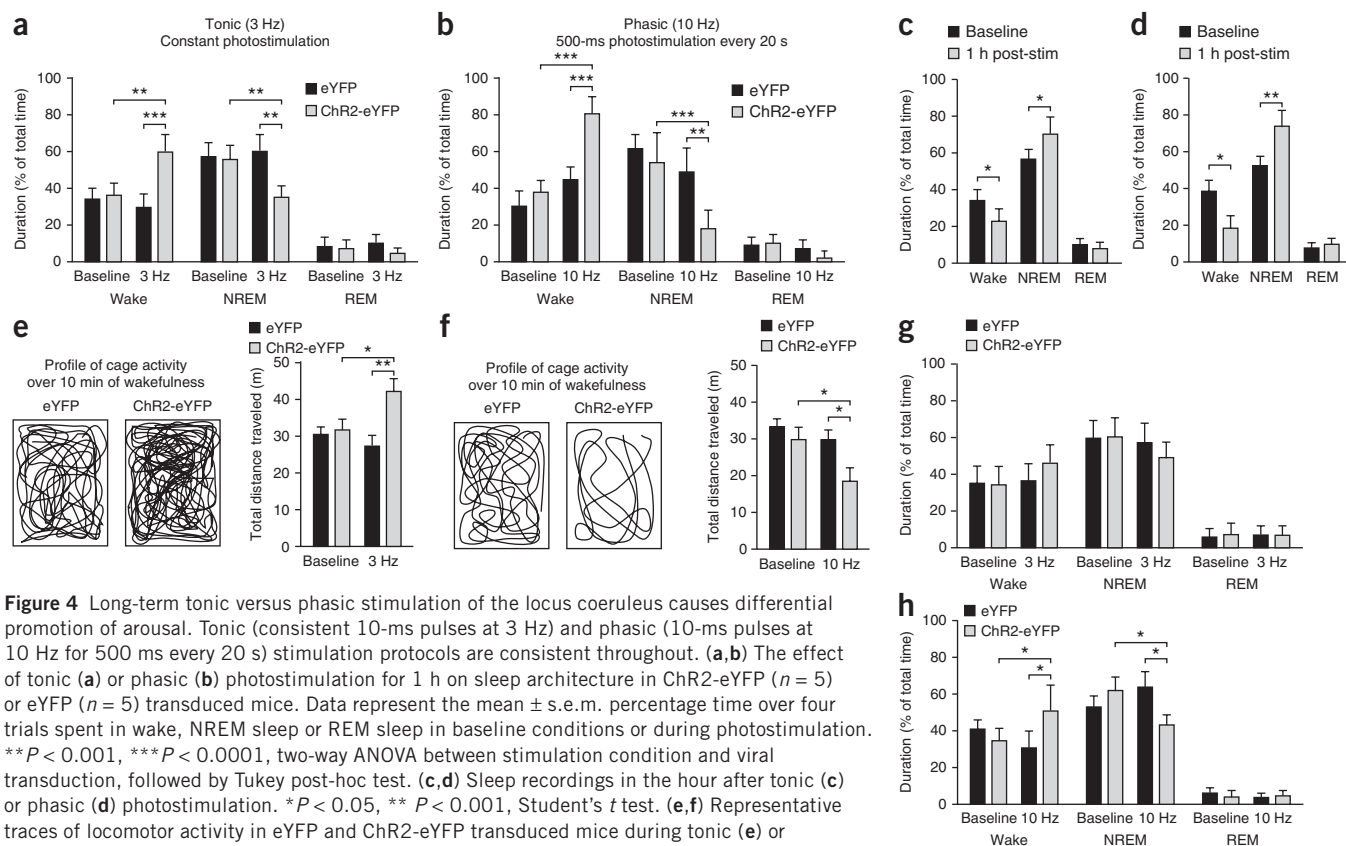

Figure 4 Long-term tonic versus phasic stimulation of the locus coeruleus causes differential promotion of arousal. Tonic (consistent 10-ms pulses at 3 Hz) and phasic (10-ms pulses at 10 Hz for 500 ms every 20 s) stimulation protocols are consistent throughout. (**a**,**b**) The effect of tonic (**a**) or phasic (**b**) photostimulation for 1 h on sleep architecture in ChR2-eYFP ($n = 5$) or eYFP ($n = 5$) transduced mice. Data represent the mean ± s.e.m. percentage time over four trials spent in wake, NREM sleep or REM sleep in baseline conditions or during photostimulation. **$P < 0.001$, ***$P < 0.0001$, two-way ANOVA between stimulation condition and viral transduction, followed by Tukey post-hoc test. (**c**,**d**) Sleep recordings in the hour after tonic (**c**) or phasic (**d**) photostimulation. *$P < 0.05$, ** $P < 0.001$, Student's t test. (**e**,**f**) Representative traces of locomotor activity in eYFP and ChR2-eYFP transduced mice during tonic (**e**) or phasic (**f**) photostimulation for 1 h during a 10-min wake period. Quantification (right) shows the mean ± s.e.m. distance traveled by eYFP ($n = 5$) or ChR2-eYFP ($n = 5$) transduced mice over the 1-h of photostimulation after 5 sessions of stimulation per mouse. *$P < 0.05$, **$P < 0.001$, two-way ANOVA between stimulation condition and viral transduction, followed by Tukey post-hoc test. (**g**,**h**) The effect of tonic (**g**) or phasic (**h**) photostimulation for 5 h on sleep architecture in ChR2-eYFP ($n = 5$) or eYFP ($n = 5$) transduced mice. *$P < 0.05$, two-way ANOVA between stimulation condition and viral transduction, followed by Tukey post-hoc test.

To determine whether sleep-to-wake transitions mediated by the locus coeruleus depend on the release of norepinephrine, we repeated photostimulation experiments (10-ms pulses at 5 Hz for 5 s) in ChR2-eYFP mice ($n = 4$) 30 min after administration of the adrenergic α2 receptor agonist clonidine or the α1 receptor antagonist prazosin, both of which suppress norepinephrine transmission. In ChR2 mice that were injected with saline, photostimulation always caused sleep-to-wake transitions (probability = 1.00). Administration of either clonidine or prazosin reduced the probability of NREM and REM sleep-to-wake transitions in a dose-dependent manner (**Supplementary Fig. 9**). These results show that sleep-to-wake transitions mediated by the locus coeruleus depend, at least in part, on normal norepinephrine transmission.

Long-term stimulation of locus coeruleus neurons

To identify the effects of long-term stimulation on arousal, we photostimulated locus coeruleus neurons for 1 h during the inactive period and measured changes in sleep-wake duration and general locomotor activity. Previous physiological recordings of the locus coeruleus showed that neurons fire tonically at 1–3 Hz during wakefulness[6-8], and also phasically in short bursts (500 ms) of 8–10 Hz during the presentation of salient stimuli that prolong wake states[7,9]. Therefore, we decided to study the effects of long-term stimulation

using both tonic and phasic stimulation to see whether these had different effects on arousal. Tonic stimulation consisted of constant 10-ms light pulses at 3 Hz, whereas phasic stimulation consisted of 10-ms pulses at 10 Hz for 500 ms (five light pulses) every 20 s.

Both tonic and phasic stimulation increased total wakefulness and decreased total NREM sleep in ChR2-eYFP mice, compared with eYFP mice ($n = 5$ mice per condition; **Fig. 4a,b**). The reduction in sleep that was caused by photostimulation of locus coeruleus neurons at tonic and phasic frequencies can be considered to be a model of sleep deprivation, as the following hour (without photostimulation) showed hallmarks of sleep pressure including a rebound of NREM sleep and a significant increase in SWA in the cortical EEG ($P < 0.05$, Student's t test between baseline and 1 h after stimulation; **Fig. 4c,d**). Tonic and phasic stimulation of locus coeruleus neurons had different effects on locomotor activity: tonic stimulation caused a significant increase in locomotor activity over the hour of stimulation ($P < 0.001$; **Fig. 4e**), whereas phasic stimulation caused a significant decrease ($P < 0.05$; **Fig. 4f**). Finally, we investigated whether tonic or phasic stimulation would increase the total duration of wakefulness over longer time periods of 5 h. We found that, unlike 1 h of stimulation, tonic stimulation at 3 Hz for 5 h did not result in a significant difference in the total duration of wakefulness or NREM sleep states between ChR2-eYFP and eYFP mice ($P > 0.05$; $n = 5$ mice per condition; **Fig. 4g**). Alternatively, phasic stimulation for 5 h resulted
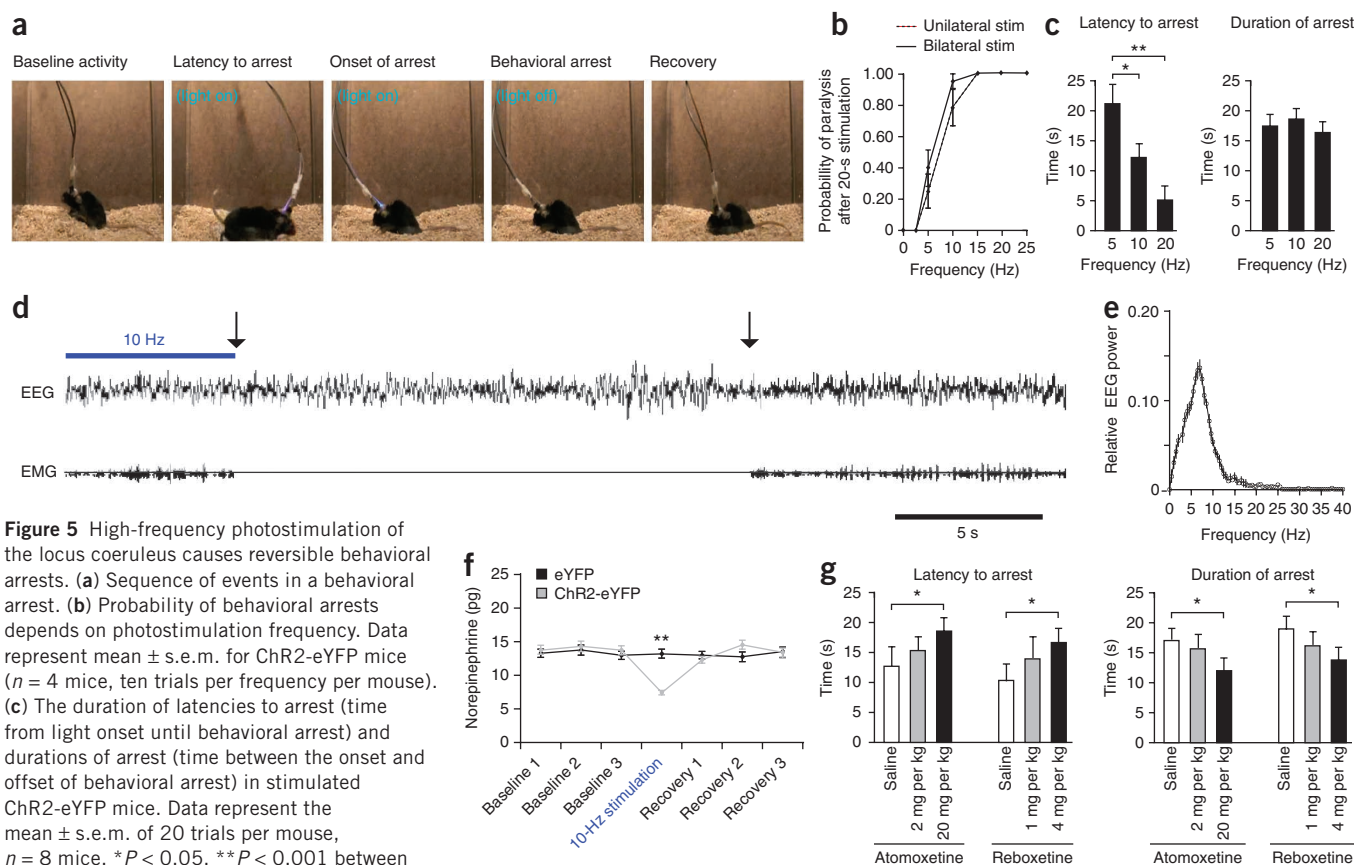

Figure 5 High-frequency photostimulation of the locus coeruleus causes reversible behavioral arrests. (**a**) Sequence of events in a behavioral arrest. (**b**) Probability of behavioral arrests depends on photostimulation frequency. Data represent mean ± s.e.m. for ChR2-eYFP mice ($n = 4$ mice, ten trials per frequency per mouse). (**c**) The duration of latencies to arrest (time from light onset until behavioral arrest) and durations of arrest (time between the onset and offset of behavioral arrest) in stimulated ChR2-eYFP mice. Data represent the mean ± s.e.m. of 20 trials per mouse, $n = 8$ mice. *$P < 0.05$, **$P < 0.001$ between frequencies, ANOVA followed by Tukey post-hoc test. (**d**) Representative EEG and EMG trace of a behavioral arrest after 10-Hz photostimulation. Arrows represent the onset and offset of immobility. (**e**) Relative EEG power of the first 10 s of behavioral arrests across multiple mice. Data represent the mean ± s.e.m. relative power of 0.5-Hz binned frequencies (20 episodes per mouse, $n = 6$ mice). (**f**) Extracellular norepinephrine content in prefrontal cortex during 10-Hz stimulation. Data represent the mean ± s.e.m. of three trials per mouse, $n = 4$ mice. **$P < 0.001$, two-way ANOVA between time point and virally-transduced animal followed by Bonferroni post-hoc test. (**g**) The duration of latencies to arrest and durations of arrest in ChR2-eYFP stimulated mice upon administration of the norepinephrine reuptake inhibitors atomoxetine and reboxetine. Data represent the mean ± s.e.m. of ten trials per mouse, $n = 4$ mice. Increased darkness of bars represents increasing pharmacological dose. *$P < 0.05$, Student's t test between saline and drug-injected mice.

in a significant increase in the total amount of wakefulness ($P < 0.05$) and a decrease in the total amount of NREM sleep (**Fig. 4h**).

Together, these results indicate that long-term, tonic stimulation of locus coeruleus neurons over 1 h causes an increase in wakefulness and general locomotor activity, but that the effects of stimulation decline over a 5-h period. Long-term, phasic stimulation of locus coeruleus neurons causes an increase in wakefulness over both 1 h and 5 h, but with a decrease in locomotor activity.

High-frequency stimulation of locus coeruleus neurons

We found that sustained photostimulation of the locus coeruleus at frequencies of 5 Hz and above caused reversible behavioral arrests (**Fig. 5a** and **Supplementary Movie 2**). At the onset of stimulation, mice showed an increase in locomotor behavior that lasted for 5–20 s and was followed by immobility. After the laser diode was switched off, mice remained immobile with their eyes open for 15–20 s and then fully recovered movement. During the behavioral arrest, mice were unresponsive to tail and toe pinches. Only stimulation frequencies of 5 Hz and above produced behavioral arrests, with a 100% probability at 15 Hz and above (**Fig. 5b**). These arrests were caused by both unilateral and bilateral photostimulation; unilateral stimulation did not produce any obvious unilateral motor effects such as turning or direction bias. The latency to arrest (time from light onset to immobility) decreased as we increased the stimulation frequency, but the stimulation frequency had no effect on the duration of arrest (time from light offset to recovery of movement; **Fig. 5c**).

We hypothesized that high-frequency stimulation of the locus coeruleus caused behavioral arrests by inducing a seizure or a severe cardiovascular response. However, we detected no signs of seizure-like spike discharge in the cortical EEG (**Fig. 5d**). Instead, theta rhythm activity was prominent in the EEG across multiple mice ($n = 6$) throughout most of the behavioral arrest episodes (**Fig. 5e**). We also found no difference in heart rate or systolic blood pressure between baseline conditions and during behavioral arrests ($n = 4$; **Supplementary Fig. 10**).

We also investigated the effect of high-frequency stimulation on the release of norepinephrine. We used *in vivo* microdialysis to sample extracellular fluid from the prefrontal cortex and found that extracellular norepinephrine was substantially lower during 10 min of continuous stimulation at 10 Hz in ChR2-eYFP mice than in eYFP mice ($n = 4$ mice per condition; **Fig. 5f**). However, there was no statistical difference between the percentage decrease in cortical norepinephrine that was elicited by 10 Hz stimulation in ChR2-eYFP mice ($n = 4$ mice), which caused behavioral arrests, and the decrease in norepinephrine that was caused by constant photoinhibition in eNpHR-eYFP mice ($n = 4$ mice; **Supplementary Fig. 6**), which did not cause behavioral arrests ($P > 0.05$, two-way ANOVA between stimulation condition and transgene expression). To determine the effects of increased extracellular norepinephrine on behavioral arrests, we stimulated ChR2-eYFP mice ($n = 4$) 30 min after administration of one of the norepinephrine reuptake inhibitors atomoxitine and reboxitine. We found a dose-dependent increase in the latency to arrest and a similar decrease in the duration of arrest (**Fig. 5g**). These results indicate that sustained, high-frequency stimulation of locus coeruleus neurons depletes norepinephrine stores and that increasing norepinephrine concentration using reuptake inhibitors attenuates the arrests.

DISCUSSION
Tuning arousal by modulating locus coeruleus neurons

We found that neural activity in the locus coeruleus is both necessary for maintaining normal durations of wakefulness and sufficient to promote immediate sleep-to-wake transitions, long-term wakefulness and an increase in locomotor arousal. Together, these results suggest that the locus coeruleus is finely tuned to influence wakefulness, with even subtle differences in stimulation frequency and duration having different effects on arousal and sleep-to-wake transitions (**Supplementary Fig. 11**). Anatomically, the locus coeruleus receives many afferent projections[2,30] and is well-positioned to receive input from hypothalamic and brainstem circuits that sense salient environmental and homeostatic stimuli[31–33], as well as information from higher cognitive circuits in the prefrontal cortex[34]. In turn, the locus coeruleus projects extensively to virtually all brain regions with the exception of the striatum[2]. Therefore, the anatomical connections of the locus coeruleus, combined with our *in vivo* behavioral results, suggest that the locus coeruleus integrates information from lower and higher neural circuits and is finely tuned to affect downstream nuclei and modulate behavior.

Although our *in vitro* recordings from locus coeruleus neurons in acute brainstem slices showed the efficiency of eNpHR-mediated photoinhibition and the reliability of 10-ms pulses of blue light in causing single spikes, we cannot be certain that these tools modulate neural activity as precisely *in vivo*. We found that inhibition of the locus coeruleus using yellow light significantly decreased cortical norepinephrine ($P < 0.001$; **Supplementary Fig. 6**) and that stimulation using blue light significantly increased the expression of the immediate early gene product c-Fos throughout the anteroposterior length of the locus coeruleus ($P < 0.001$; **Supplementary Fig. 5**). However, we cannot be certain that these tools efficiently inhibit or stimulate single action potentials in awake, behaving mice. At the same time, our results clearly show effects that vary linearly with the frequency and duration of stimulation (**Supplementary Fig. 8**). Therefore, we conclude that the locus coeruleus is finely tuned to influence behavior depending on different stimulation parameters.

Previous studies in which the locus coeruleus was pharmacologically lesioned[10–12] or norepinephrine transmission was genetically ablated[13] found no substantial effect on the durations of sleep and wakefulness. By contrast, the duration of wake episodes was significantly decreased during 1 h of eNpHR-mediated inhibition of the locus coeruleus during the active period ($P < 0.05$; **Fig. 2**). A great advantage of eNpHR over traditional pharmacological or genetic loss-of-function methods is its ability to silence neural activity at specifically defined temporal windows with minimal disturbance to the animal. Perhaps permanently ablating locus coeruleus neurons or norepinephrine synthesis causes the brain to adapt using other wake-promoting systems[4], as has been reported for other brain circuits, such as those involved in food intake[35,36]. Furthermore, our rAAV-mediated genetic targeting of the locus coeruleus was able to bilaterally transduce >98% of locus coeruleus neurons, a higher percentage than previous studies using radiofrequency pulses[10], saporin[12] or DSP-4 (ref. 37). Therefore, our loss-of-function approach achieved not only acute temporal specificity but also efficient genetic targeting of the locus coeruleus, which might explain the difference between our results and those of other studies.

Inhibition of the locus coeruleus mediated by eNpHR caused a decrease in the duration of wakefulness and an increase in slow-wave activity in the EEG power spectrum at the end of wake episodes (**Fig. 2**). However, inhibition did not prevent sleep-to-wake transitions or increase the duration of sleep episodes. Unlike inhibition, stimulation of the locus coeruleus caused immediate sleep-to-wake transitions (**Fig. 3**). Therefore, we conclude that the locus coeruleus is sufficient to promote sleep-to-wake transitions, but that other nuclei must contribute to sleep-to-wake transitions in a way that is statistically redundant with locus coeruleus activity. Other known arousal-promoting

nuclei include the histaminergic tuberomammilary nucleus (TMN)[38], the serotoninergic dorsal raphe nuclei[39], the cholinergic pedunculopontine nucleus and lateral tegmental nucleus[40,41] and multiple cell types in the basal forebrain[42]. Perhaps the locus coeruleus has a more prominent, necessary role in promoting wakefulness when the animal is already awake, but is sufficient to promote arousal in a way that is redundant with other arousal systems when the animal is asleep.

Notably, naturally occurring tonic and phasic stimulation patterns had different effects on arousal (**Fig. 4**). Long-term tonic stimulation for 1 h caused an increase in the duration of wakefulness, as well as an increase in locomotor activity; however, it did not increase the duration of wakefulness during 5 h of stimulation. By contrast, long-term phasic stimulation increased the duration of wakefulness over periods of both 1 h and 5 h, but decreased locomotor activity. In the rat and primate locus coeruleus, tonic activity is correlated with wakefulness, with firing frequencies of 3 Hz during active wakefulness, 1–2 Hz during quiet wakefulness and <1 Hz during NREM sleep, with no firing during REM sleep[6–8]. Phasic activity in the locus coeruleus correlates with salient environmental stimuli[7,9] and has been proposed to underlie mechanisms of attention and behavioral or cognitive adaptation to changing environmental circumstances[1,2,5,43–45]. Therefore, it is possible that tonic stimulation at low frequencies (3 Hz) specifically causes an increase in arousal, whereas phasic frequencies might also cause changes in cortical networks and synaptic plasticity that alter cognition or attention, resulting in the loss of exploratory or locomotor behavior. Furthermore, the presentation of phasic stimulation without environmental stimuli that cause endogenous phasic activation of the locus coeruleus might confound cortical networks and result in a lack of locomotion.

Tonic and phasic frequencies are also thought to have different effects on different categories of noradrenergic receptors[1,2,44]: norepinephrine has the highest affinity for α2-receptors, which are found on both presynaptic and postsynaptic terminals and have hyperpolarizing effects. Norepinephrine has lower affinities for the α1- and β-receptors, which are primarily postsynaptic. Therefore, low, tonic release of norepinephrine might preferentially activate α2-receptors, whereas high-frequency, phasic release of norepinephrine may preferentially activate α1- and β-receptors. Perhaps tonic stimulation of locus coeruleus neurons promotes wakefulness for 1 h, but is insufficient to increase arousal at longer time periods owing to steady activation of α2-receptors, which leads to self-inhibition of the locus coeruleus and inhibition of downstream targets. Alternatively, phasic stimulation of locus coeruleus neurons may cause long-term activation of α1- and β-receptors, allowing mice to maintain wakefulness over longer time periods.

The locus coeruleus can cause behavioral arrests

An unexpected finding of our study was that sustained high frequency (>5 Hz) stimulation of the locus coeruleus causes reversible behavioral arrests (**Fig. 5**). We hypothesized that these arrests were caused by seizure or a severe cardiovascular response, but found no signs of seizure-like spike discharge in the cortical EEG or statistically significant differences in heart rate or blood pressure ($P > 0.05$; **Fig. 5e** and **Supplementary Fig. 10**).

When we used microdialysis to sample extracellular fluid from the cortex, we found that high-frequency stimulation of the locus coeruleus caused a decrease in cortical norepinephrine (**Fig. 5f**), suggesting that high-frequency, non-physiological levels of stimulation depleted norepinephrine from locus coeruleus terminals. Unfortunately, microdialysis has a temporal resolution of several minutes, preventing detection of norepinephrine discharge rates over the 10–15 s of high-frequency stimulation that is necessary to cause behavioral arrests.

Voltammetry techniques have better temporal resolution but are not good at distinguishing between norepinephrine and other catecholamines. We hypothesize that high-frequency stimulation of the locus coeruleus causes a rapid increase in extracellular norepinephrine over several seconds, followed by the decrease that was measured by microdialysis. The decrease in norepinephrine could be due to a breakdown of cortical norepinephrine in the synapse and the inability of locus coeruleus terminals to replenish norepinephrine while still firing at >5-Hz stimulation. When blue light stimulation ceased, the locus coeruleus terminals could replenish norepinephrine stores, allowing the animal to recover. Indeed, increasing extracellular norepinephrine by preventing reuptake attenuated the arrests (**Fig. 5f**).

However, behavioral arrests cannot be caused solely by a decrease in brain norepinephrine, as eNpHR-mediated inhibition produced statistically similar decreases in cortical norepinephrine concentrations without causing arrests (**Supplementary Fig. 6**). Furthermore, previous studies in which locus coeruleus activity was ablated did not produce behavioral arrests[10–12]. The inability of photoinhibition to cause arrests may be due to the synergistic effects of other neuromodulatory systems. For example, serotonin cell activity (and presumably serotonin release) is greatly decreased in cataplexy[46] and REM sleep[47]. Thus, inhibiting the locus coeruleus during tonic activity in raphe neurons may allow muscle tone to be maintained by serotonin. Microdialysis studies have shown that the release of GABA and glycine release is increased when muscle tone is suppressed[48], which causes active inhibition in motor neurons. Excessive firing of norepinephrine neurons may trigger the activity of postsynaptic inhibitory neurons in the brainstem and thereby elicit a behavioral arrest.

Behavioral arrests may be caused by nonendogenous release of norepinephrine onto noradrenergic receptors. As discussed above, α1- and β-receptors may be preferentially activated by phasic rather than tonic frequencies. Therefore, the high-frequency stimulation that elicits behavioral arrests mediated by the locus coeruleus may cause marked, nonendogenous activation of α1- and β-receptors, followed by a relative loss of extracellular norepinephrine as indicated by our microdialysis results (**Fig. 5f**). This rapid release followed by depletion at postsynaptic terminals is an unexplored phenomenon, and future *in vitro* research using slice preparations is necessary to understand the consequences of a rapid efflux of norepinephrine at postsynaptic sites.

The behavioral arrests described here may represent the symptoms of some neuropsychiatric disorders with no known etiology. Behavioral arrests mediated by the locus coeruleus are not inconsistent with a mouse model of cataplexy defined by the International Working Group on Rodent Models of Narcolepsy[49]. This condition is generally defined by an abrupt episode of nuchal atonia lasting at least 10 s and an EEG characteristic of theta activity, with at least 40 s of wakefulness preceding the episode. The behavioral arrests mediated by the locus coeruleus that we have characterized here fit these criteria (**Fig. 5**). However, locus coeruleus-mediated arrests are likely to be analogous rather than homologous to mouse cataplexy, as the locus coeruleus has been shown to be silent before cataplectic attacks[50] rather than showing the high-frequency activity described here. Nevertheless, our results might necessitate a revision of the consensus definition of cataplexy, and it will be important for future studies to consider the role of the locus coeruleus in mediating the symptoms of other neuropsychiatric diseases.

METHODS

Methods and any associated references are available in the online version of the paper at http://www.nature.com/natureneuroscience/.

Note: Supplementary information is available on the Nature Neuroscience website.

AUTHOR CONTRIBUTIONS

M.E.C. and L.d.L. designed the study and wrote the manuscript. M.E.C. performed or assisted with all experiments. O.Y. performed and analyzed electrophysiology experiments, S.C. performed HPLC analysis, and H.N. analyzed immunohistochemical co-expression data. A.A. and L.d.L. provided expertise on optogenetic and polysomnographic recording techniques, as well as substantial feedback on the manuscript. S.N., K.D. and L.d.L. provided equipment, reagents and critical feedback.

COMPETING FINANCIAL INTERESTS

The authors declare no competing financial interests.

Published online at http://www.nature.com/natureneuroscience/.
Reprints and permissions information is available online at http://www.nature.com/reprintsandpermissions/.

1. Aston-Jones, G. & Cohen, J.D. An integrative theory of locus coeruleus-norepinephrine function: adaptive gain and optimal performance. *Annu. Rev. Neurosci.* **28**, 403–450 (2005).
2. Berridge, C.W. & Waterhouse, B.D. The locus coeruleus-noradrenergic system: modulation of behavioral state and state-dependent cognitive processes. *Brain Res. Brain Res. Rev.* **42**, 33–84 (2003).
3. Foote, S.L., Bloom, F.E. & Aston-Jones, G. Nucleus locus ceruleus: new evidence of anatomical and physiological specificity. *Physiol. Rev.* **63**, 844–914 (1983).
4. Saper, C.B., Scammell, T.E. & Lu, J. Hypothalamic regulation of sleep and circadian rhyhms. *Nature* **437**, 1257–1263 (2005).
5. Sara, S.J. The locus coeruleus and noradrenergic modulation of cognition. *Nat. Rev. Neurosci.* **10**, 211–223 (2009).
6. Aston-Jones, G. & Bloom, F.E. Activity of norepinephrine-containing locus coeruleus neurons in behaving rats anticipates fluctuations in the sleep-waking cycle. *J. Neurosci.* **1**, 876–886 (1981).
7. Aston-Jones, G. & Bloom, F.E. Norepinephrine-containing locus coeruleus neurons in behaving rats exhibit pronounced responses to non-noxious environmental stimuli. *J. Neurosci.* **1**, 887–900 (1981).
8. Hobson, J.A., McCarley, R.W. & Wyzinski, P.W. Sleep cycle oscillation: reciprocal discharge by two brainstem neuronal groups. *Science* **189**, 55–58 (1975).
9. Foote, S.L., Aston-Jones, G. & Bloom, F.E. Impulse activity of locus coeruleus neurons in awake rats and monkeys is a function of sensory stimulation and arousal. *Proc. Natl. Acad. Sci. USA* **77**, 3033–3037 (1980).
10. Jones, B.E., Harper, S.T. & Halaris, A.E. Effects of locus coeruleus lesions upon cerebral monoamine content, sleep-wakefulness states and the response to amphetamine in the cat. *Brain Res.* **124**, 473–496 (1977).
11. Lidbrink, P. The effect of lesions of ascending noradrenaline pathways on sleep and waking in the rat. *Brain Res.* **74**, 19–40 (1974).
12. Blanco-Centurion, C., Gerashchenko, D. & Shiromani, P.J. Effects of saporin-induced lesions of three arousal populations on daily levels of sleep and wake. *J. Neurosci.* **27**, 14041–14048 (2007).
13. Hunsley, M.S. & Palmiter, R.D. Norepinephrine-deficient mice exhibit normal sleep-wake states but have shorter sleep latency after mild stress and low doses of amphetamine. *Sleep* **26**, 521–526 (2003).
14. Berridge, C.W. & Espana, R.A. Synergistic sedative effects of noradrenergic alpha(1)- and beta-receptor blockade on forebrain electroencephalographic and behavioral indices. *Neuroscience* **99**, 495–505 (2000).
15. De Sarro, G.B., Ascioti, C., Froio, F., Libri, V. & Nistico, F. Evidence that locus coeruleus is the site where clonidine and drugs acting at alpha 1- and alpha 2-adrenoceptors affect sleep and arousal mechanisms. *Br. J. Pharmacol.* **90**, 675–685 (1987).
16. Flicker, C. & Geyer, M.A. The hippocampus as a possible site of action for increased locomotion during intracerebral infusions of norepinephrine. *Behav. Neural Biol.* **34**, 421–426 (1982).
17. Segal, D.S. & Mandell, A.J. Behavioral activation of rats during intraventricular infusion of norepinephrine. *Proc. Natl. Acad. Sci. USA* **66**, 289–293 (1970).
18. Berridge, C.W. & Foote, S.L. Effects of locus coeruleus activation on electroencephalographic activity in neocortex and hippocampus. *J. Neurosci.* **11**, 3135–3145 (1991).
19. Gradinaru, V. *et al.* Targeting and readout strategies for fast optical neural control *in vitro* and *in vivo. J. Neurosci.* **27**, 14231–14238 (2007).
20. Zhang, F., Aravanis, A.M., Adamantidis, A., de Lecea, L. & Deisseroth, K. Circuit-breakers: optical technologies for probing neural signals and systems. *Nat. Rev. Neurosci.* **8**, 577–581 (2007).
21. Adamantidis, A., Zhang, F., Aravanis, A.M., Deisseroth, K. & de Lecea, L. Neural substrates of awakening probed with optogenetic control of hypocretin neurons. *Nature* **450**, 420–424 (2007).
22. Carter, M.E., Adamantidis, A., Ohtsu, H., Deisseroth, K. & de Lecea, L. Sleep homeostasis modulates hypocretin-mediated sleep-to-wake transitions. *J. Neurosci.* **29**, 10939–10949 (2009).
23. Gradinaru, V., Thompson, K.R. & Deisseroth, K. eNpHR: a Natronomonas halorhodopsin enhanced for optogenetic applications. *Brain Cell Biol.* **36**, 129–139 (2008).
24. Zhang, F. *et al.* Multimodal fast optical interrogation of neural circuitry. *Nature* **446**, 633–639 (2007).
25. Boyden, E.S., Zhang, F., Bamberg, E., Nagel, G. & Deisseroth, K. Millisecond-timescale, genetically targeted optical control of neural activity. *Nat. Neurosci.* **8**, 1263–1268 (2005).
26. Sohal, V.S., Zhang, F., Yizhar, O. & Deisseroth, K. Parvalbumin neurons and gamma rhythms enhance cortical circuit performance. *Nature* **459**, 698–702 (2009).
27. Tsai, H.C. *et al.* Phasic firing in dopaminergic neurons is sufficient for behavioral conditioning. *Science* **324**, 1080–1084 (2009).
28. Lindeberg, J. *et al.* Transgenic expression of Cre recombinase from the tyrosine hydroxylase locus. *Genesis* **40**, 67–73 (2004).
29. Paxinos, G. & Franklin, K. *The Mouse Brain in Stereotaxic Coordinates.* 2nd edn. (Academic, New York, 2001).
30. Shipley, M.T. *et al.* Dendrites of locus coeruleus neurons extend preferentially into two pericoerulear zones. *J. Comp. Neurol.* **365**, 56–68 (1996).
31. Bourgin, P. *et al.* Hypocretin-1 modulates rapid eye movement sleep through activation of locus coeruleus neurons. *J. Neurosci.* **20**, 7760–7765 (2000).
32. Valentino, R. *et al.* Corticotropin-releasing factor innervation of the locus coeruleus region: distribution of fibers and sources of input. *Neuroscience* **48**, 689–705 (1992).
33. van Bockstaele, E.J. *et al.* Anatomic basis for differential regulation of the rostrolateral peri-locus coeruleus region by limbic afferents. *Biol. Psychiatry* **46**, 1352–1363 (1999).
34. Jodo, E., Chiang, C. & Aston-Jones, G. Potent excitatory influence of prefrontal cortex activity on noradrenergic locus coeruleus neurons. *Neuroscience* **83**, 63–79 (1998).
35. Luquet, S., Perez, F.A., Hnasko, T.S. & Palmiter, R.D. NPY/AgRP neurons are essential for feeding in adult mice, but can be ablated in neonates. *Science* **310**, 683–685 (2005).
36. Wu, Q., Boyle, M.P. & Palmiter, R.D. Loss of GABAergic signaling by AgRP neurons to the parabrachial nucleus leads to starvation. *Cell* **137**, 1225–1234 (2009).
37. Szot, P. *et al.* A comprehensive analysis of the effect of DSP4 on the locus coeruleus noradrenergic system in the rat. *Neuropharmacology* **166**, 279–291 (2010).
38. Parmentier, R. *et al.* Anatomical, physiological, and pharmacological characteristics of histidine decarboxylase knock-out mice: evidence for the role of brain histamine in behavioral and sleep-wake control. *J. Neurosci.* **22**, 7695–7711 (2002).
39. McGinty, D.J. & Harper, R.M. Dorsal raphe neurons: depression of firing during sleep in cats. *Brain Res.* **101**, 569–575 (1976).
40. Steriade, M. Acetycholine systems and rhythmic activities during the waking-sleep cycle. *Prog. Brain Res.* **145**, 179–196 (2004).
41. Boucetta, S. & Jones, B.E. Activity profiles of cholinergic and intermingled GABAergic and putative glutamatergic neurons in the pontomesencelphalic tegmentum of urethane-anesthetized rats. *J. Neurosci.* **29**, 4664–4674 (2009).
42. Hassani, O.K., Lee, M.G., Henny, P. & Jones, B.E. Discharge profiles of identified GABAergic in comparison to cholinergic and putative glutamatergic basal forebrain neurons across the sleep-wake cycle. *J. Neurosci.* **29**, 11828–11840 (2009).
43. Arnsten, A.F. Stress signaling pathways that impair prefrontal cortex structure and function. *Nat. Rev. Neurosci.* **10**, 410–422 (2009).
44. Ramos, B.P. & Arnsten, A. Adrenergic pharmacology and cognition: focus on the prefrontal cortex. *Pharmacol. Ther.* **113**, 523–536 (2007).
45. Bouret, S. & Sara, S.J. Network reset: a simplified overarching theory of locus coeruleus noradrenaline function. *Trends Neurosci.* **28**, 574–582 (2005).
46. Wu, M.F. *et al.* Activity of dorsal raphe cells across the sleep-waking cycle and during cataplexy in narcoleptic dogs. *J. Physiol. (Lond.)* **554**, 202–215 (2004).
47. Lai, Y.Y., Kodama, T. & Siegel, J.M. Changes in monoamine release in the ventral horn and hypoglossal nucleus linked to pontine inhibition of muscle tone: an *in vivo* microdialysis study. *J. Neurosci.* **21**, 7384–7391 (2001).
48. Kodama, T., Lai, Y.Y. & Siegel, J.M. Changes in inhibitory amino acid release linked to pontine-induced atonia: an *in vivo* microdialysis study. *J. Neurosci.* **23**, 1548–1554 (2003).
49. Scammell, T.E. *et al.* A consensus definition of cataplexy in mouse models of narcolepsy. *Sleep* **32**, 111–116 (2009).
50. Wu, M.F. *et al.* Locus coeruleus neurons: cessation of activity during cataplexy. *Neuroscience* **91**, 1389–1399 (1999).

ONLINE METHODS

Mice. Tyrosine hydroxylase (TH)∷IRES-Cre knockin mice[28] (EM:00254) were obtained from the European Mouse Mutant Archive and mated with c57Bl/6 wild-type mice. We used only male heterozygous mice, aged 8–10 weeks at the start of experimental procedures and no more than 18 weeks at the end of experimental procedures. Mice were housed in individual plexiglass recording chambers in custom-designed stainless steel cabinets at constant temperature (22 ± 1 °C), humidity (40–60%), and circadian cycle (12 h light-dark cycle, starting at 9:00 a.m.). Food and water were available *ad libitum*. All experiments were performed in accordance with the guidelines described in the US National Institutes of Health *Guide for the Care and Use of Laboratory Animals*.

Virus preparation. Cre-inducible recombinant AAV vectors carrying optogenetic transgenes were serotyped with AAV5 coat proteins and packaged by the viral vector core at the University of North Carolina. The final viral concentration was 2×10^{12} genome copies (gc) per ml. Aliquots of virus were stored at −80 °C before stereotaxic injection.

Surgery. At the start of surgical procedures, mice were anesthetized with ketamine and xylazine anesthesia (80 and 16 mg per kg of body weight, respectively, intra-peritoneal injection) and placed on a small animal stereotaxic frame (David Kopf Instruments). Recombinant AAV5 carrying Ef1α∷eNpHR-eYFP, Ef1α∷ChR2-eYFP or control Ef1α∷eYFP was unilaterally or bilaterally injected adjacent to the locus coeruleus (anteroposterior (AP), 5.45 mm; mediolateral (ML), ± 1.28 mm; dorsoventral (DV) 3.65 mm)[29] through an internal cannula (Plastics One) at a rate of 0.1 µl min^{-1} for 10 min (1 µl total volume; **Supplementary Fig. 1**). Mice that received unilateral injections were used for initial viral expression experiments (**Fig. 1**) and no further surgical procedures took place. Mice that received bilateral injections were used for all other experiments and received additional surgical implants, described below.

After viral injection, mice received surgical implantation of a 26G bilateral cannula (Plastics One) with 2 mm between individual cannulae and 3 mm shaft length (**Supplementary Fig. 3**). The cannula was placed above the locus coeruleus (AP, 5.45 mm; ML, ± 1.0 mm; DV, 3.0 mm) and affixed to the skull with C&B Metabond (Parkell) and dental acrylic.

Mice used for sleep recordings were also implanted with a custom-made EEG-EMG implant placed anterior to the cannula (**Supplementary Fig. 3**). EEG signals were recorded from electrodes on the frontal (AP, −2 mm; ML, ± 2.5 mm) and temporal (AP, 3 mm; ML, ± 2.5 mm) cortices. EMG signals were recorded from two electrodes inserted in the neck musculature to record postural tone.

After surgical procedures, mice were allowed to recover in individual housing for at least 2 weeks. Mice used for sleep recordings were then acclimated to a flexible EEG-EMG connection cable for an additional 7 d within individual recording chambers. Each cable was flexible so that mice could freely move about their cages. Fiber optic cables were implanted at least 2 d before experiments and ran alongside the EEG-EMG connection cables (**Supplementary Fig. 3**).

Electrophysiology. Acute brainstem coronal slices (250 µm) were collected on a vibratome and prepared as described[21]. Transduced locus coeruleus neurons were identified by eYFP fluorescence. Whole-cell recordings were conducted using a Multiclamp 700B and signals were digitized at 10 kHz.

Polysomnographic recording and analysis. All sleep recordings took place between 12:00 and 18:00 (light onset at 9:00) except for photoinhibition experiments in the active (dark) period, which took place between 21:00 and 24:00 (light offset at 21:00). EEG and EMG signals derived from the surgically implanted electrodes were amplified (Grass Instruments) and digitized at 256 Hz using sleep recording software (Vital Recorder, Kissei Comtec America). The signals were digitally filtered and spectrally analyzed by fast Fourier transformation, and poly-somnographic recordings were scored using sleep analysis software (SleepSign for Animal, Kissei Comtec America). All scoring was performed manually based on the visual signature of the EEG and EMG waveforms, as well as the power spectra of 5-s epochs.

We defined wakefulness as desynchronized low-amplitude EEG and height-ened tonic EMG activity with phasic bursts. We defined NREM sleep as synchro-nized, high-amplitude, low-frequency (0.5–4 Hz) EEG and highly reduced EMG activity compared with wakefulness with no phasic bursts. We defined REM sleep

as having a pronounced theta rhythm (4–9 Hz) and a flat EMG. All sleep-scoring was done by an investigator (M.E.C.) blind to the viral transgene delivered to the animal and to baseline versus stimulation or inhibition conditions.

Photostimulation and photoinhibition. All photostimulation experiments except for c-Fos expression analysis (**Supplementary Fig. 5**) were conducted bilaterally. Fiber optic cables (2 m long, 200 µm diameter; ThorLabs) were placed inside the implanted cannulae 2 h before stimulation or inhibition experiments. Mice were allowed at least 2 d to acclimatize before experimental sessions. For photostimulation experiments, light pulse trains (10-ms pulses of various frequency and duration; see text) were programmed using a waveform generator (33220A Waveform Generator, Agilent Technologies) that provided simultaneous input into two blue-light lasers (473 nm, 20 mW light intensity; LaserGlo). For acute photostimulation experiments, each stimulation epoch was applied 15 s after a stable NREM or REM sleep event as detected by real-time online EEG-EMG analysis. For photoinhibition experiments, light delivery was provided by a yellow-light laser (593 nm; LaserGlo) split into two fiber optic cables.

Cardiovascular measurements. We measured heart rate and blood pressure in mice during photostimulation experiments using a tail cuff attached to a MK-2000ST Blood Pressure Monitor for Mice (Muromachi). Mice were accli-mated to a mouse holder and blood pressure was measured at a starting pressure of 50 mm Hg.

Microdialysis and high pressure liquid chromatography. Mice used for micro-dialysis experiments (**Fig. 5** and **Supplementary Fig. 6**) were surgically implanted with a microdialysis cannula (EICOM) with 1 mm shaft length. The cannulae were placed in prefrontal cortex (AP, 1.5 mm; ML, 0.5 mm; DV, 1 mm) and affixed to the skull with C&B Metabond and dental acrylic.

During experiments, a microdialysis probe (EICOM) with 1-mm membrane length was placed in the guide cannula and the mouse was allowed a 30-min acclimation period before perfusion. During collection, we continuously perfused fresh artificial cerebrospinal fluid (aCSF: 147 mM NaCl, 2.8 mM KCl, 1.2 mM CaCl$_2$, 1.2 mM MgCl$_2$ in H$_2$0) at a rate of 1 µl min^{-1} for 10 min for each sample. Dialysates were collected into chilled 0.5-ml tubes containing 10 µl aCSF with 0.02 M acetic acid. Each experimental session lasted 70 min: 3×10 min for base-line measurements, 1×10 min for measurements during photostimulation with 10 Hz blue light (**Fig. 5**) or inhibition with yellow light (**Supplementary Fig. 6**), and 3×10 min recovery measurements.

Norepinephrine levels in the dialysate were determined by HPLC with elec-trochemical detection. Microdialysis samples (10 µl dialysate and 10 µl aCSF with 0.02 M acetic acid) were mixed with 20 µl 0.1 M acetic acid containing 0.27 mM EDTA. Samples were injected using an autoinjector (Bio-Rad). The HPLC mobile phase (0.1 M sodium phosphate buffer, 0.13 mM EDTA, 2.3 mM 1-octanesulfonic acid, 7% MeOH, pH 6.0) was pumped through a chromatography column (SC-5ODS, EICOM) and a 20-µl sample loop at a flow rate of 0.23 ml min^{-1}. A graphite electrode set (WE-3G, EICOM) at a potential of 460 mV was used for electrochemical detection and quantified with a PowerChrom analy-sis system (ADInstruments) using external norepinephrine standards (Sigma). Norepinephrine concentrations were calculated by comparing the HPLC peak of norepinephrine in each sample with the peak area of known concentrations of the standards analyzed on the same day.

Histology. After completion of experiments, mice were anesthetized with keta-mine and xylazine anesthesia (80 and 16 mg per kg, respectively, intraperitoneal injection) and perfused transcardially with 1× PBS, pH 7.4, followed by 4% para-formaldehyde in PBS. The brains were extracted, allowed to postfix overnight in the same fixative at 4 °C, and cryoprotected in 30% sucrose dissolved in 1× PBS for an additional 24 h at 4 °C. Each brain was sectioned at 30 µm on a cryostat (Leica Microsystems) and collected in cold PBS.

For colocalization experiments (**Fig. 1a** and **Supplementary Fig. 2**), brain sections from eYFP transduced mice were washed in PBS with 0.3% Triton X-100 (PBST) for 10 min at room temperature. Sections were then incubated in a blocking solution composed of PBST with 4% bovine serum albumin and 2% normal horse serum for 1 h at room temperature. For primary antibody expo-sure, sections were incubated in chicken anti-tyrosine hydroxylase (1:2,000, Aves

Labs, #TH) in block solution at 4 °C for ~16 h. After 3 × 10-min washes in PBST, sections were incubated in Alexa Fluor 568 goat anti-chicken IgG secondary antibody (1:500, Molecular Probes, #A-11041) in block solution for 1 h at room temperature. Sections were washed 3 times in 1× PBS, mounted onto SuperFrost Plus glass slides (VWR, #48311-703), and coverslipped with VECTASHIELD with DAPI Mounting Media (Vector Laboratories, #H-1200). Quantification of colocalization was performed on adjacent sections from approximately bregma −5.20 to −5.80 (exactly 21 sections per mouse).

For c-Fos experiments (**Supplementary Fig. 5a**), brain sections from eYFP and ChR2-eYFP transduced mice were washed in PBST and incubated in a 3% hydrogen peroxide solution for 30 min at room temperature. After a brief wash in PBST, sections were incubated in block solution for 1 h at room temperature. Sections were incubated in rabbit anti-c-Fos (1:5,000, Calbiochem, #PC05) in block solution at 4 °C for approximately 16 h. After 3 × 10-min washes in PBST, sections were incubated in biotinylated goat anti-rabbit IgG secondary antibody (1:500, Vector Laboratories, #BA-1000) for 1 h at room temperature. Next, the sections were washed 3 × 10 min in PBST and incubated in an avidin-biotin ABC peroxidase solution (Vector Laboratories, #PK-6100) for 30 min at room tempera-ture. Finally, the sections were washed 3 × 10 min in 1× PBS and stained using 3-3′diaminobenzidine-4 HCl (DAB) and nickel solution (Vector Laboratories, SK-4100) to produce a black staining product.

After this initial round of staining for the presence of c-Fos, sections were sub-mitted to a second round of staining for tyrosine hydroxylase. After a brief wash in PBST, sections were incubated in chicken anti-tyrosine hydroxylase (1:2,000, Aves Labs, #TH) in block solution at 4 °C for approximately 16 h. Following 3 × 10-min washes in PBST, sections were incubated in biotinylated goat

anti-chicken IgG secondary antibody (1:500, Vector Laboratories, #BA-9010) for 1 h at room temperature. Next, the sections were washed 3 × 10 min in PBST and incubated in an avidin-biotin ABC peroxidase solution (Vector Laboratories, #PK-6100) for 30 min at room temperature. Finally, the sections were washed 3 × 10 min in 1× PBS and stained using DAB alone to produce a brown staining product. After 3 × 5 min washes in 1× PBS, processed sections were mounted onto slides and coverslipped using Permaslip (Alban Scientific). As in viral expression experiments, colocalization of c-Fos immunofluorescence (black) and tyrosine hydroxylase immunofluorescence (brown) was quantified on adjacent sections from approximately bregma −5.20 to −5.80 (exactly 21 sections total per mouse). Tyrosine hydroxylase-positive cells were scored for the presence of c-Fos by an investigator (M.E.C.) blind to the side of stimulation and identity of the virally-transduced mouse (eYFP or ChR2-eYFP).

Microscopy. Non-confocal images were collected on a Carl Zeiss fluorescent microscope either using fluorescent reflected light (**Fig. 1a** and **Supplementary Fig. 2**) or brightfield transmitted light (**Supplementary Fig. 5a**). Confocal images (**Fig. 1a**) were collected on a Zeiss LSM 510 Meta confocal microscope. Digital images were minimally processed using Adobe Photoshop CS3 (Adobe Systems) to enhance brightness and contrast for optimal representation of the data. All digital images were processed in the same way between experimental conditions to avoid artificial manipulation between different datasets.

Statistics. All data were analyzed using Prism 5.0 (GraphPad Software) as described in the text. Data were exported into Adobe Illustrator CS3 (Adobe Systems) for preparation of figures.